Int. J. Heat Mass Transfer. Vol. 8, pp. 815–831. Pergamon Press 1965. Printed in Great Britain

LAMINAR FREE CONVECTION ALONG A VERTICAL PLATE AT EXTREMELY SMALL GRASHOF NUMBERS

FRANCIS J. SURIANO,* KWANG-TZU YANG† and JEROME A. DONLON‡
Department of Mechanical Engineering, University of Notre Dame, Notre Dame, Indiana

(*Received* 5 *August* 1964 *and in revised form* 2 *November* 1964)

Abstract—Laminar free convection in the vicinity of an isothermal vertical finite plate is studied in the Grashof-number range between zero and unity and two Prandtl numbers of 0·72 and 10·0, by means of a perturbation analysis. Solutions to the governing differential equations are expressed in perturbation series with the Grashof number itself taken as the perturbation parameter. Three terms in all series expansions have been calculated numerically by using the relaxation technique for both Prandtl numbers. Results of all perturbation functions, as well as of isothermal and stream lines for various Grashof numbers and the two Prandtl numbers are shown graphically and discussed. Finally, these results are used to discuss the leading-edge effects relative to the well-known boundary-layer solutions.

NOMENCLATURE

G, $= g\beta L^3(\bar{T}_w - \bar{T}_\infty)/\nu^2$, Grashof number;
g, gravitational acceleration;
h, coefficient of heat transfer;
k, fluid thermal conductivity;
L, height of vertical plate;
N, $= hL/k$, Nusselt number;
N_0, limiting Nusselt number at $G = 0$;
p, $= (\bar{p} - \bar{p}_\infty)L^2/\rho\nu^2$;
$\bar{p}$, static pressure;
$\bar{T}$, temperature;
u, $= \bar{u}L/\nu$;
$\bar{u}$, velocity component in the $\bar{x}$-direction;
v, $= \bar{v}L/\nu$;
$\bar{v}$, velocity component in the $\bar{y}$-direction;
x, $= \bar{x}/L$;
$\bar{x}$, coordinate along the plate measured from the mid-point, positive in the direction against gravity;
x_m, location of matching along the plate;
y, $= \bar{y}/L$;
$\bar{y}$, coordinate normal to the plate measured from the plate.

Greek symbols

α, fluid thermal diffusivity;
β, fluid coefficient of volumetric expansion;
δ, square grid size;
θ, $= (\bar{T} - \bar{T}_\infty)/(\bar{T}_w - \bar{T}_\infty)$;
ν, fluid kinematic viscosity;
ρ, fluid density;
σ, fluid Prandtl number;
ψ, dimensionless stream function;
∇^2, Laplacian operator in Cartesian co-ordinate system.

Subscripts

w, wall conditions;
∞, conditions in the environment.

Superscripts

(0), (1), (2),..., orders of perturbations.

INTRODUCTION

FREE-CONVECTION studies have received much attention in the recent heat-transfer literature. For laminar free convection in the vicinity of heated surfaces, the majority of analytical investigations, by far, deal with boundary-layer phenomena. Mathematically, these boundary-layer solutions represent asymptotic solutions to the governing partial differential equations as

* Graduate Research Assistant.
† Professor.
‡ Graduate Research Assistant, presently Graduate N.I.H. Fellow, Department of Radiation Biology and Biophysics, University of Rochester.

the kinematic viscosity approaches zero, or the Grashof number tends to infinity. In practice, these solutions do give satisfactory physical results when the Grashof number becomes sufficiently high. It is perhaps evident that such external free-convection phenomena cannot be considered as completely understood without the corresponding physical knowledge in the rest of the Grashof-number range, namely, the range of moderate and small Grashof numbers. Even though many experimental correlations on the overall rates of heat transfer for different geometries are known in the literature, they, however, fail to give any insight to the interaction between the momentum and energy fields, and as to how this interaction is affected by changing Grashof and Prandtl numbers. Much less is known analytically. In the range of moderately high Grashof numbers, Yang and Jerger [1] recently obtained a perturbation solution for laminar free-convection boundary layers along a finite and isothermal vertical plate, from which detailed first-order deviations from the classical Pohlhausen solution have been evaluated. Their results in local velocity profiles compare better with the experimental data of Schmidt and Beckmann [2] than that of the pure boundary-layer solution. However, their predicted correction on the overall rate of heat transfer at the plate surface, though very small, bears a different sign as that according to the existing experimental correlations. In the range of low Grashof numbers, no detailed results for any geometry are known in the literature. Farzetdinov [3] suggested a perturbation solution in this range and proved a uniqueness theorem for this solution. Zeroth-order approximation in this perturbation solution is taken to be that of steady conduction. Earlier, Mahony [4], in dealing with heat transfer at low Grashof numbers from thin wires and spheres, utilized independently the same perturbation series, and obtained some qualitative results by directly matching the steady-conduction solution to asymptotic similarity solutions for wake flows valid at large distances from the heat source. The flow field was not considered. Also, it may be pertinent here to mention the study by Reeves and Kippenhan [5] who showed the existence of a similarity solution to the complete set of governing partial differential equations for laminar free convection along a vertical plate where the surface temperature varies linearly with the distance away from the leading edge, and is valid for all Grashof and Prandtl numbers. This solution is identical to that obtainable from the boundary-layer equations [6], and does not, however, correspond to any realistic physical condition when the Grashof number goes to zero, and hence is only of academic interest. In view of the above, it is perhaps quite evident that much remains to be done in this area of research.

The primary purpose of this study is to attempt to provide some detailed information concerning the steady momentum and energy fields in the range of extremely small Grashof numbers. In view of the great complexity of the governing differential equations, a simple geometry of a vertical finite plate with a uniform surface temperature has been chosen for this study. The present approach is also based on perturbation series expansions as independently suggested by Mahony [4] and Farzetdinov [3], utilizing the Grashof number itself as the perturbation parameter. All perturbation functions in the zeroth-, first- and second-order approximations, which are governed by elliptic equations, are calculated in detail for two Prandtl numbers of 0·72 and 10·0, by means of standard relaxation technique. The results are shown to be valid in the Grashof-number range between zero and unity.

Before the mathematical formulation of the present problem is described, it is of particular interest to mention an additional incentive to studying this problem. It arises from the results of the boundary-layer perturbation solution given by Yang and Jerger [1]. As already noted previously, they have shown that their first-order perturbations in the momentum field do account for the deviations in local velocity profiles from the classic boundary-layer solution, as compared to the experimental data. However, their predicted Nusselt numbers, contrary to the experimental data, fall below that according to the classical solution. It has been suggested [1] that this slight discrepancy could result from the inadequacy of the boundary-layer perturbation solution to take into account the relatively strong convection effect in the immediate

vicinity of the leading edge as a result of leading-edge conduction. Since the leading-edge phenomenon is essentially a low Grashof-number phenomenon, the validity of the above conjecture can only be determined after the low Grashof-number solution to the problem is available. Such a determination has also been attempted in the present study and result will be shown later in the paper.

FORMULATION AND THE PRESENT APPROACH

For steady laminar free convection in the vicinity of a two-dimensional finite vertical plate maintained at a uniform temperature different from that in the environment, the governing Navier–Stokes equations of motion, continuity equation and energy equation may be respectively written as

$$\bar{u}\frac{\partial \bar{u}}{\partial \bar{x}} + \bar{v}\frac{\partial \bar{u}}{\partial \bar{y}} = -\frac{1}{\rho}\frac{\partial \bar{p}}{\partial \bar{x}} + g\beta(\bar{T} - \bar{T}_\infty) + \nu\nabla^2\bar{u} \tag{1}$$

$$\bar{u}\frac{\partial \bar{v}}{\partial \bar{x}} + \bar{v}\frac{\partial \bar{v}}{\partial \bar{y}} = -\frac{1}{\rho}\frac{\partial \bar{p}}{\partial \bar{y}} + \nu\nabla^2\bar{v} \tag{2}$$

$$\frac{\partial \bar{u}}{\partial \bar{x}} + \frac{\partial \bar{v}}{\partial \bar{y}} = 0 \tag{3}$$

$$\bar{u}\frac{\partial \bar{T}}{\partial \bar{x}} + \bar{v}\frac{\partial \bar{T}}{\partial \bar{y}} = \alpha\nabla^2\bar{T} \tag{4}$$

where $\bar{x}$ is the coordinate along the plate, measured from the mid-point on the plate and positive in the direction against the gravity, and $\bar{y}$ is the normal coordinate measured from the plate. The unknowns are the velocity components $\bar{u}$ and $\bar{v}$, the static pressure $\bar{p}$, and the temperature $\bar{T}$. It is noted that the plate leading edge is located at $\bar{x} = -L/2$ and $\bar{y} = 0$. Other symbols are defined in the Nomenclature. In these equations, the usual conditions of constant property values except slight change in density, negligible static-pressure gradient in the environment and negligible viscous dissipation have also been utilized. The associated boundary conditions are as follows:

$$\left.\begin{aligned}
&\bar{x} \to \pm\infty \quad \bar{u} = \bar{v} \to 0 \quad \bar{p} \to \bar{p}_\infty \\
&\qquad\qquad \bar{T} \to \bar{T}_\infty \quad \text{any } \bar{y} \\
&\bar{y} = 0 \quad \bar{x} > \frac{L}{2} \text{ and } \bar{x} < -\frac{L}{2} \\
&\qquad\qquad \frac{\partial \bar{u}}{\partial \bar{y}} = \bar{v} = \frac{\partial \bar{p}}{\partial \bar{y}} = \frac{\partial \bar{T}}{\partial \bar{y}} = 0 \\
&-\frac{L}{2} \leqslant \bar{x} \leqslant \frac{L}{2} \quad \bar{u} = \bar{v} = 0 \\
&\qquad\qquad \bar{T} = \bar{T}_w \text{ (constant)} \\
&\bar{y} \to +\infty \quad \bar{u} = \bar{v} \to 0 \quad \bar{p} \to \bar{p}_\infty \\
&\qquad\qquad \bar{T} \to \bar{T}_\infty \quad \text{any } \bar{x}
\end{aligned}\right\} \tag{5}$$

where L is the total height of the plate. Note that it is only necessary to consider the half plane $y \geqslant 0$ in view of symmetry. In order to bring out the characteristic dimensionless quantities in the problems, it is desirable to re-cast the above equations in dimensionless forms. By introducing the following definitions:

$$u = \frac{\bar{u}L}{\nu} \quad v = \frac{\bar{v}L}{\nu} \quad x = \frac{\bar{x}}{L} \quad y = \frac{\bar{y}}{L}$$

$$\theta = \frac{\bar{T} - \bar{T}_\infty}{\bar{T}_w - \bar{T}_\infty} \quad p = \frac{(\bar{p} - \bar{p}_\infty)L^2}{\rho\nu^2}$$

$$G = \frac{g\beta(\bar{T}_w - \bar{T}_\infty)L^3}{\nu^2}$$

Equations (1), (2), (3) and (4) reduce to

$$u\frac{\partial u}{\partial x} + v\frac{\partial u}{\partial y} = -\frac{\partial p}{\partial x} + G\theta + \nabla^2 u \tag{6}$$

$$u\frac{\partial v}{\partial x} + v\frac{\partial v}{\partial y} = -\frac{\partial p}{\partial y} + \nabla^2 v \tag{7}$$

$$\frac{\partial u}{\partial x} + \frac{\partial v}{\partial y} = 0 \tag{8}$$

$$u\frac{\partial \theta}{\partial x} + v\frac{\partial \theta}{\partial y} = \frac{1}{\sigma}\nabla^2\theta \tag{9}$$

respectively, and the boundary conditions (5) in turn become

$$\left.\begin{aligned}
&x \to \pm\infty \quad u = v \to 0 \quad p \to 0 \quad \theta \to 0 \quad \text{any } y \\
&y = 0 \quad x > \tfrac{1}{2} \text{ and } x < -\tfrac{1}{2} \\
&\qquad\qquad \frac{\partial u}{\partial y} = v = \frac{\partial p}{\partial y} = \frac{\partial \theta}{\partial y} = 0
\end{aligned}\right\} \tag{10}$$

$$\left.\begin{array}{l} -\frac{1}{2} \leqslant x \leqslant \frac{1}{2} \quad u = v = 0 \quad \theta = 1 \\ y \to +\infty \quad u = v \to 0 \quad p \to 0 \quad \theta \to 0 \quad \text{any } x \end{array}\right\} \quad (10)$$

It is evident that the only parameters in this problem are the Grashof number G and the Prandtl number σ.

In the present study, a perturbation solution to equations (6) to (10) is sought in the following forms:

$$\left.\begin{aligned} \theta &= \theta^{(0)} + G\theta^{(1)} + G^2\theta^{(2)} + \ldots . \\ u &= Gu^{(1)} + G^2u^{(2)} + \ldots . \\ v &= Gv^{(1)} + G^2v^{(2)} + \ldots . \\ p &= Gp^{(1)} + G^2p^{(2)} + \ldots . \end{aligned}\right\} \quad (11)$$

where all perturbation functions are dependent of the space variables and the Prandtl number. For sufficiently small Grashof numbers, these expansions are expected to converge satisfactorily [3]. When equations (11) are substituted into equations (6–9) and terms with like powers of G are collected, the following equations governing the perturbation functions are obtained:

The zeroth-order approximation:

$$\nabla^2\theta^{(0)} = 0 \quad (12)$$

The first-order approximations:

$$\nabla^2u^{(1)} - \frac{\partial p^{(1)}}{\partial x} = -\theta^{(0)} \quad (13)$$

$$\nabla^2v^{(1)} - \frac{\partial p^{(1)}}{\partial y} = 0 \quad (14)$$

$$\frac{\partial u^{(1)}}{\partial x} + \frac{\partial v^{(1)}}{\partial y} = 0 \quad (15)$$

$$\frac{\partial \theta^{(0)}}{\partial x}u^{(1)} + \frac{\partial \theta^{(0)}}{\partial y}v^{(1)} = \frac{1}{\sigma}\nabla^2\theta^{(1)} \quad (16)$$

The second-order approximations:

$$\nabla^2u^{(2)} - \frac{\partial p^{(2)}}{\partial x} = u^{(1)}\frac{\partial u^{(1)}}{\partial x} + v^{(1)}\frac{\partial u^{(1)}}{\partial y} - \theta^{(1)} \quad (17)$$

$$\nabla^2v^{(2)} - \frac{\partial p^{(2)}}{\partial y} = u^{(1)}\frac{\partial v^{(1)}}{\partial x} + v^{(1)}\frac{\partial v^{(1)}}{\partial y} \quad (18)$$

$$\frac{\partial u^{(2)}}{\partial x} + \frac{\partial v^{(2)}}{\partial y} = 0 \quad (19)$$

$$u^{(1)}\frac{\partial \theta^{(1)}}{\partial x} + u^{(2)}\frac{\partial \theta^{(0)}}{\partial x} + v^{(1)}\frac{\partial \theta^{(1)}}{\partial y} + v^{(2)}\frac{\partial \theta^{(0)}}{\partial y} = \frac{1}{\sigma}\nabla^2\theta^{(2)} \quad (20)$$

A few observations can be made at this time. The limiting temperature distribution as Grashof number approaches zero, which is that of pure conduction, is independent of the Prandtl number. Consequently, as the Grashof or Rayleigh number tends to zero, the Nusselt numbers based on the average coefficient of heat transfer and height of the plate for different Prandtl numbers converge to the same limiting value. This characteristic agrees well with existing experimental data. Also, the Prandtl number does not influence the momentum field, as represented by $u^{(1)}$, $v^{(1)}$ and $p^{(1)}$, when the Grashof number is exceedingly small, such that G^2-terms are negligible.

Before the corresponding boundary conditions are listed, it is convenient in the present approach to cast some of the perturbation equations in somewhat different forms. For the first-order perturbations, the continuity equation (15) can be replaced by another equation obtained by differentiating equation (13) with respect to x and equation (14) with respect to y, and then adding the resulting equations with the help of (15). This equation may now be written as

$$\nabla^2p^{(1)} = \frac{\partial \theta^{(0)}}{\partial x} \quad (21)$$

Similarly, equation (19) may be eliminated, and in its place we have

$$\nabla^2p^{(2)} = \frac{\partial \theta^{(1)}}{\partial x} - 2\left[\frac{\partial v^{(1)}}{\partial x}\frac{\partial u^{(1)}}{\partial y} + \left(\frac{\partial u^{(1)}}{\partial x}\right)^2\right] \quad (22)$$

Here it is noted that all perturbation equations, equation (12) for the zeroth-order approximation, equations (14), (21), (13) and (16) for the first-order approximations, equations (18), (22), (17) and (20) for the second-order approximations, and so on, are linear and of the elliptic type, and consequently they may be solved by

the same approach. Specific boundary conditions may be readily derived from equations (10), and are listed as follows:

The zeroth-order approximation:

$$y = 0 \qquad x > \tfrac{1}{2} \text{ and } x < -\tfrac{1}{2} \qquad \frac{\partial \theta^{(0)}}{\partial y} = 0$$

$$-\tfrac{1}{2} \leqslant x \leqslant \tfrac{1}{2} \qquad \theta^{(0)} = 1$$

$$y \to \infty \qquad \theta^{(0)} \to 0 \qquad \text{any } x$$

$$x \to \pm \infty \qquad \theta^{(0)} \to 0 \qquad \text{any } y$$

The first-order approximations:

$$y = 0 \quad x > \tfrac{1}{2} \text{ and } x < -\tfrac{1}{2} \quad v^{(1)} = \frac{\partial u^{(1)}}{\partial y} = \frac{\partial p^{(1)}}{\partial y} = \frac{\partial \theta^{(1)}}{\partial y} = 0$$

$$-\tfrac{1}{2} \leqslant x \leqslant \tfrac{1}{2} \quad u^{(1)} = v^{(1)} = \frac{\partial v^{(1)}}{\partial y} = \theta^{(1)} = 0$$

$$y \to \infty \qquad u^{(1)} = v^{(1)} = p^{(1)} = \theta^{(1)} \to 0 \quad \text{any } x$$

$$x \to \pm \infty \quad u^{(1)} = v^{(1)} = p^{(1)} = \theta^{(1)} \to 0 \quad \text{any } y$$

The second-order approximations:

$$y = 0 \quad x > \tfrac{1}{2} \text{ and } x < -\tfrac{1}{2} \quad v^{(2)} = \frac{\partial u^{(2)}}{\partial y} = \frac{\partial p^{(2)}}{\partial y} = \frac{\partial \theta^{(2)}}{\partial y} = 0$$

$$-\tfrac{1}{2} \leqslant x \leqslant \tfrac{1}{2} \quad u^{(2)} = v^{(2)} = \frac{\partial v^{(2)}}{\partial y} = \theta^{(2)} = 0$$

$$y \to \infty \qquad u^{(2)} = v^{(2)} = p^{(2)} = \theta^{(2)} \to 0 \quad \text{any } x$$

$$x \to \pm \infty \quad u^{(2)} = v^{(2)} = p^{(2)} = \theta^{(2)} \to 0 \quad \text{any } y$$

On the plate, the conditions

$$\frac{\partial v^{(1)}}{\partial y} = \frac{\partial v^{(2)}}{\partial y} = 0$$

are obtained from the continuity equation and are necessary in view of the increased order of pressure derivatives. For the same reason, equations (14) and (21) are coupled, and so are equations (18) and (22). Solutions to these perturbation equations for a given Prandtl number proceed in the following order: Equation (12) is first solved, followed by simultaneous solutions to equations (14) and (21) for $v^{(1)}$ and $p^{(1)}$. Then $u^{(1)}$ is obtained from equation (13). To complete the first-order approximations, equation (16) is then solved for $\theta^{(1)}$. Solutions to the second-order perturbation equations and so on follow the same order as that in the first-order approximations.

In view of the complexity of these equations, any simplification is desirable. Since $\theta^{(0)}$ represents the forcing function in all subsequent perturbations, and is symmetrical with respect to the y-axis, this property of symmetry is carried into all the other functions. Once these properties of symmetry are known, it is then only necessary to carry out the solutions to the perturbation equations in the quarter plane, instead of in the half plane as noted previously. These symmetry properties can be analyzed easily by considering the signs of the inhomogeneous parts for $x > 0$ and $x < 0$. For instance, consider equation (21) for $p^{(1)}$. The inhomogeneous part $(\partial\theta^{(0)}/\partial x)$ is symmetrical relative to the y-axis in magnitude, but changes sign going from $x > 0$ to $x < 0$. Consequently, $p^{(1)}$ is expected to be also symmetrical with respect to $x = 0$ in magnitude, but has different signs in the two regions. On this basis, it may be readily shown that all perturbation functions are symmetrical relative to the y-axis in magnitude, and the corresponding sign relations are those given in Table 1, where the boxed quantities in the region $x < 0$ are those which bear different signs as the corresponding quantities in the region $x > 0$.

Table 1. Symmetry properties of perturbation functions

$x > 0$	$\theta^{(0)}$	$p^{(1)}$ $u^{(1)}$	$v^{(1)}$ $\theta^{(1)}$	$p^{(2)}$ $u^{(2)}$	$v^{(2)}$ $\theta^{(2)}$
$x < 0$	$\theta^{(0)}$	$\boxed{p^{(1)}}$ $u^{(1)}$	$\boxed{v^{(1)}}$ $\boxed{\theta^{(1)}}$	$p^{(2)}$ $\boxed{u^{(2)}}$	$v^{(2)}$ $\theta^{(2)}$

It is perhaps evident that in the quarter-plane solutions of the perturbation equations, the boundary conditions along $x = 0$ are such that either the particular perturbation function under consideration is zero in the case when it has different signs in the two regions $x > 0$ and

$x < 0$, or its first derivative with respect to x is zero, when it has same signs in both regions.

In the present study, all perturbation equations up to and including those in the second-order approximations have been calculated numerically on a UNIVAC-1107 digital computer by means of the standard relaxation technique [7]. Some details of the calculations are described in the next section.

NUMERICAL CALCULATIONS

In the numerical calculations, a square-grid system in the quarter plane $x \geqslant 0$ and $y \geqslant 0$, with a grid size of δ, has been used in the relaxation solution. The difference equations, which can be easily derived and are not presented here for simplicity, are known to involve errors of the order of δ^4. In order to be consistent with this degree of accuracy, all derivatives appearing in the inhomogeneous parts of the perturbation equations are evaluated by five-point differentiation formulae [8], which also involve errors of the order of δ^4. A grid size of 0·125, such that the entire plate is divided into eight intervals, has been chosen. In view that a change in δ to $\delta = 0{\cdot}0625$ hardly changes the solution for the zeroth-order approximation, this smaller grid size was used in the zeroth-order approximation, and the grid size of $\delta = 0{\cdot}125$ is used throughout the rest of the calculations.

The locations of infinity in both space-coordinate directions are determined by extending the grid system out in these directions until the calculated perturbation functions approach their respective values at infinity asymptotically. For both Prandtl numbers of 0·72 and 10·0, it has been found that locations of infinity may be represented by $x = \pm 7{\cdot}5$ and $y = 7{\cdot}0$, noting that the plate height is represented by unity. Consequently, it is seen that approximately 3200 grid points in the quarter plane are treated in the calculation of each perturbation function.

The allowable residue in any set of relaxation calculation may be found by satisfying the conditions that its value becomes only a small fraction of the maximum value of the unknown quantity under consideration, and that a significant change in the value of the residue does not produce a correspondingly significant change in the unknown. However, actual values used for the maximum allowable residues, for practical reasons, depend primarily on whether further reduction in residue would require excessive machine time on the computer. For both Prandtl numbers, the achieved ratio of the maximum residue to the maximum value of the quantity under calculation is 0·12 per cent for $\theta^{(0)}$, 0·20 per cent for $p^{(1)}$, $v^{(1)}$, $u^{(1)}$ and $\theta^{(1)}$, 2·0 per cent for the perturbation functions in the second-order approximations. Higher-order residue values or inaccuracy can be tolerated in the second-order approximations for two reasons. One is that, as noted previously, no higher-order approximations are attempted, and consequently the accuracy in the second-order quantities does not become critical. Secondly, the first-order perturbation functions are considerably larger than the corresponding second-order quantities, and hence in the small Grashof-number range considered in this study the second-order approximations do not contribute greatly toward the magnitudes of the physical variables at a specific Grashof number.

Furthermore, it may be of interest to mention that in all relaxation calculations no difficulty has been encountered relative to the convergence of calculations when the residues are successively reduced. However, one exception is in the simultaneous relaxation calculations for $p^{(2)}$ and $v^{(2)}$, where divergence has been observed whenever one allowable residue proportionately becomes significantly different from the other. This difficulty, however, was easily corrected when both residues were allowed to reduce successively in same, but small percentages.

RESULTS AND DISCUSSIONS

The zeroth-order heat conduction solution for the quarter plane $x \geqslant 0$ and $y \geqslant 0$ is shown in Fig. 1 in terms of isothermal lines. The leading and trailing edges of the vertical plate are singularities where temperatures are discontinuous. However, in the numerical solutions they are considered to be integral parts of the plate, and consequently the discontinuities are smoothed out. It is noted that this solution is valid, insofar as the numerical calculations are concerned, for plates of any thickness, as long as the thickness is less than the grid size δ. Since $\theta^{(0)}$ represents the limiting temperature

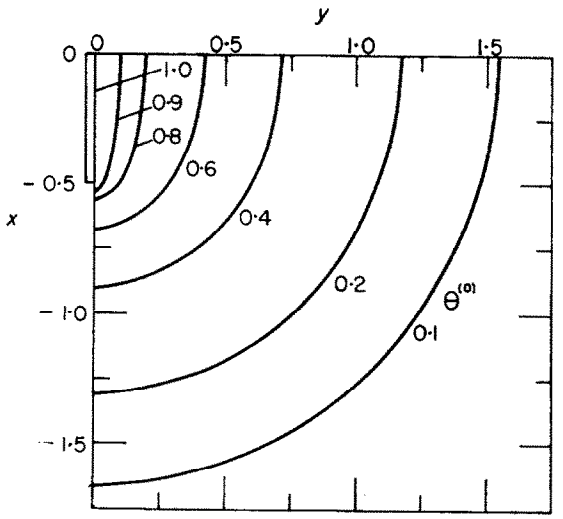

FIG. 1. Limiting temperature field $\theta^{(0)}$.

field as the Grashof number tends to zero, the corresponding rate of heat transfer at the surface gives the limiting Nusselt number N_0 as described by

$$N_0 = \frac{hL}{k} = \int_{-1/2}^{1/2} \left[-\frac{\partial \theta^{(0)}}{\partial y} \right] dx \qquad (23)$$

where h and k are the average coefficient of heat transfer and fluid thermal conductivity, respectively. According to the presently calculated $\theta^{(0)}$, N_0 is given by a value of 1·4413. It is of particular interest to compare this value with several existing experimental correlations. Jakob [9] has suggested a corresponding limiting value of 0·4 based on correlations involving a good variety of geometries. However, there is an indication that the value for vertical plates is somewhat higher. In fact, according to the correlation of McAdams [10] dealing specifically with short vertical plates, the Nusselt number at a Rayleigh number of unity is given by 1·45. Since the present results indicate, as will be shown later, that the Nusselt number does not vary much in the region $0 \leqslant G \leqslant 1{\cdot}0$, especially for the lower Prandtl number of 0·72, the limiting value of 1·4413 obtained here could be considered in good agreement with McAdam's correlation. Also, for comparison purpose, a more recent correlation by Buznik and Bezlonstsev [11] suggests a limiting value of 1·0 for a horizontal plate.

The first-order perturbation functions $p^{(1)}$, $v^{(1)}$, $u^{(1)}$ and $\theta^{(1)}$ are respectively shown in Figs. 2, 3, 4 and 5 for several values of x in the quarter plane $x \leqslant 0$ and $y \geqslant 0$. The corresponding behaviors for $x > 0$ can be readily deduced from symmetry as indicated in Table 1. The perturbation functions $p^{(1)}$, $v^{(1)}$ and $u^{(1)}$ are specifically independent of Prandtl number, and physically describe the initial momentum field when the Grashof number deviates slightly from zero. In such an instance, the Grashof number is but a scale factor in influencing the momentum field. Based on these results, several observations concerning the physical phenomenon can be made. In the neighborhood of the leading edge of the plate, static pressures fall below that at infinity. The decrease in the negative x-direction reach a minimum at about one plate length below the leading edge, and then increase asymptotically to the environment pressure as $x \to -\infty$. Along the plate, the pressure gradient remains positive. These behaviors may be compared to that of the boundary layers where the pressure gradient is zero throughout the flow field. Also in the neighborhood of the leading edge, the velocity component $u^{(1)}$ is always positive, while $v^{(1)}$ remains negative. This indicates the fact that the fluid particles are drawn in toward the plate due to heating from the plate. As soon as these same particles get into the region $x > 0$, they tend to move away from the plate, since in this region $u^{(1)}$ remains positive, while $v^{(1)}$ changes sign. The velocity profiles in Fig. 4 are of special interest. Along the plate, they behave very similarly to the well-known boundary-layer profiles. In fact, this similarity is even carried into the wake region above the plate [12], where the velocity profile changes into the familiar bell shape. However, quantitatively there is a very important difference between the asymptotic wake flow at distances far from the heat source, based on the boundary-layer equations and that obtained here, which is based on the complete set of governing equations (1), (2), (3) and (4). According to the boundary-layer solution, as given by [12] and others, the centerline velocity increases without bound as distance from the heat source increases, while

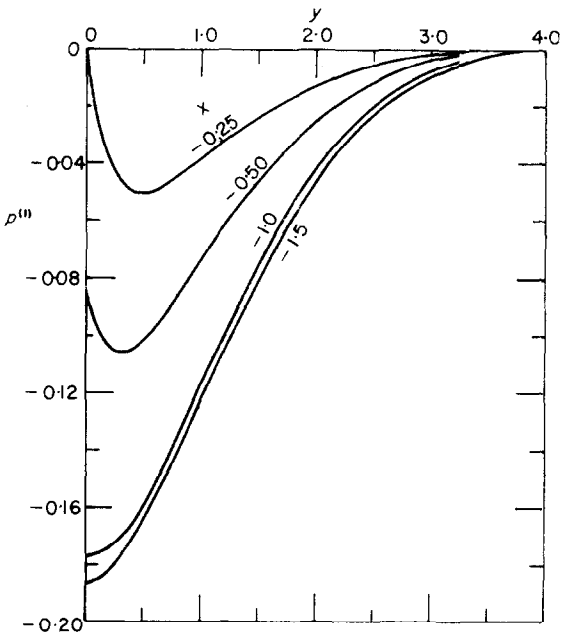

FIG. 2. First-order pressure perturbation $p^{(1)}$.

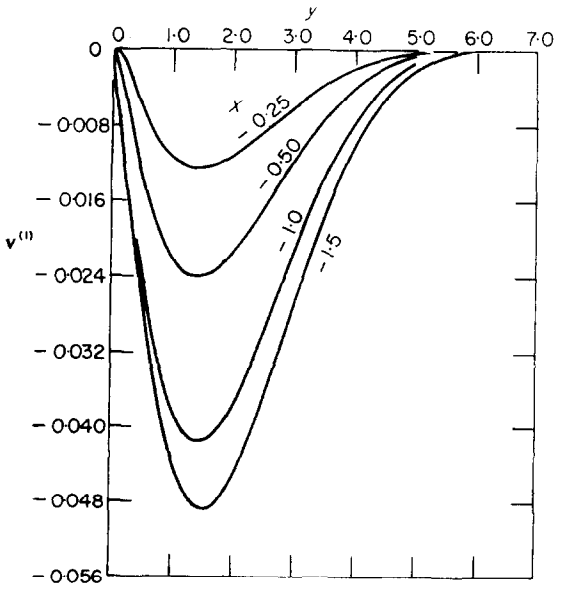

FIG. 3. First-order normal-velocity perturbation $v^{(1)}$.

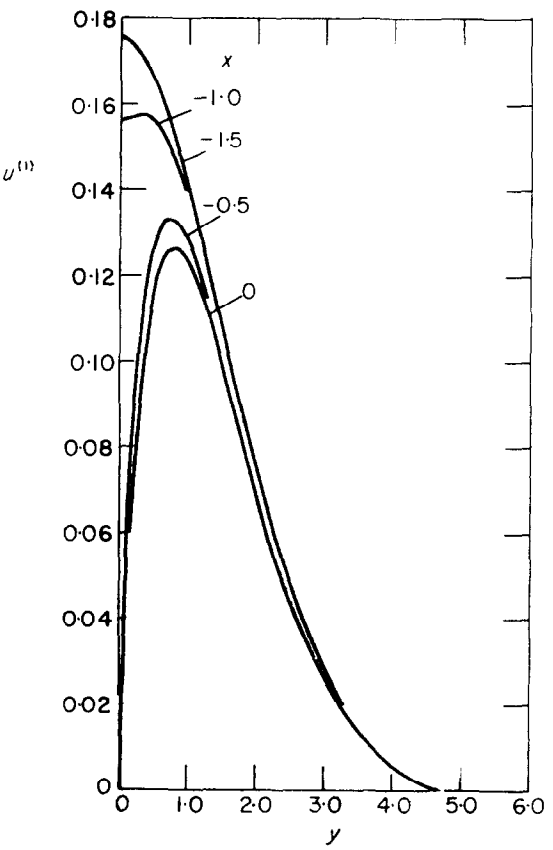

FIG. 4. First-order velocity perturbatoin $u^{(1)}$.

according to the present result, the centerline velocity goes through a maximum and then decreases asymptotically to zero at infinity, a condition which must be satisfied in a physically realistic case. The difficulty with the boundary-layer formulation is that it grossly under-estimates the effect of the normal velocity component in the wake region. This becomes even more obvious when the corresponding streams lines, which will be shown later, are examined. Also of particular interest is the relation between the magnitudes of $u^{(1)}$ and $v^{(1)}$ in the immediate neighborhood of the plate for positive x. It is seen here that $u^{(1)}$ is considerably larger than $v^{(1)}$ even in this region of low Grashof numbers. A reasonable conjecture is that as the Grashof number increases, the normal velocity component v is to decrease monotonically relative

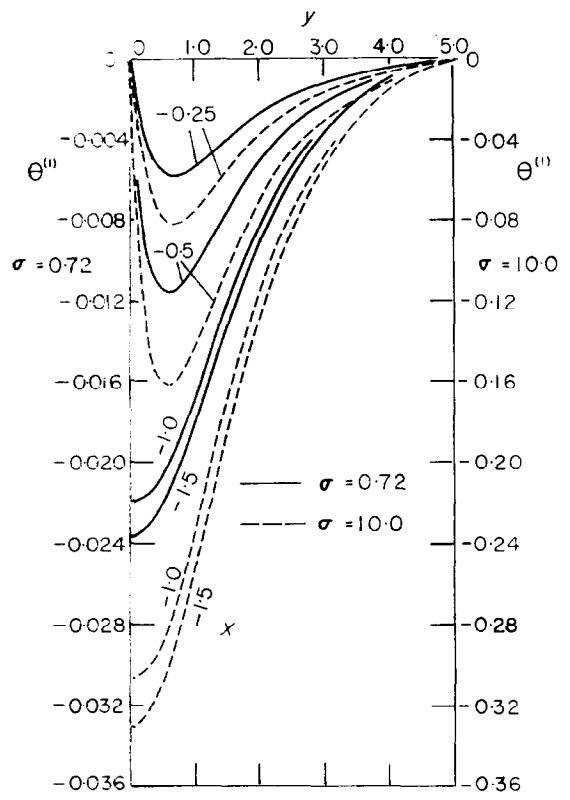

FIG. 5. First-order temperature perturbation $\theta^{(1)}$ for Prandtl numbers 0·72 and 10·0.

to u until eventually the ratio v/u attains the order of magnitude of $G^{-1/4}$, according to the boundary-layer theory. The first-order perturbation of the temperature field as given by $\theta^{(1)}$ in Fig. 5 for both Prandtl numbers does not directly represent a physical phenomenon. However, its contribution toward the temperature field for Grashof numbers deviating slightly from zero is quite significant, and can be physically explained without difficulty. In the lower half plane, regardless of Prandtl number $\theta^{(1)}$ is negative and its sign is reversed for $x > 0$ in accordance with Table 1. Consequently for a Grashof number other than zero in this range of extremely small Grashof numbers, the temperatures are reduced in the lower-half plane, but increased in the upper-half plane, when compared to the temperature field for $G = 0$ (Fig. 1). This is evidently due to the convection effect as a result of $u^{(1)}$ and $v^{(1)}$, which carry thermal energy from the lower-half plane to the upper-half plane. This effect is seen to be more pronounced for the higher Prandtl-number fluid. Also, it is significant to note that in view of the symmetry of $\theta^{(1)}$ relative to $x = 0$, the first-order perturbation does not contribute at all toward the average rate of heat transfer from the plate, or the average Nusselt number. Consequently, in order to determine the Nusselt number–Rayleigh number relationship for a given Prandtl number in the present analysis, the second-order perturbation functions must be considered.

All second-order perturbation functions are dependent on the Prandtl number, and have been calculated for both Prandtl numbers of 0·72 and 10·0. They are shown graphically in Figs. 6 to 13, inclusive, again for the quarter plane $x \leqslant 0$ and $y \geqslant 0$. The complete behaviors may again be inferred on the basis of symmetry properties indicated in Table 1. These functions only have physical meanings when they are interpreted according to equations (11).

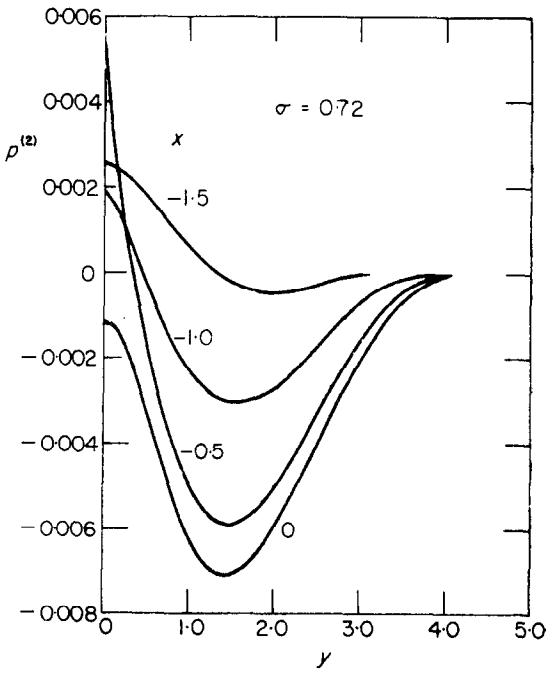

FIG. 6. Second-order pressure perturbation $p^{(2)}$ for Prandtl number 0·72.

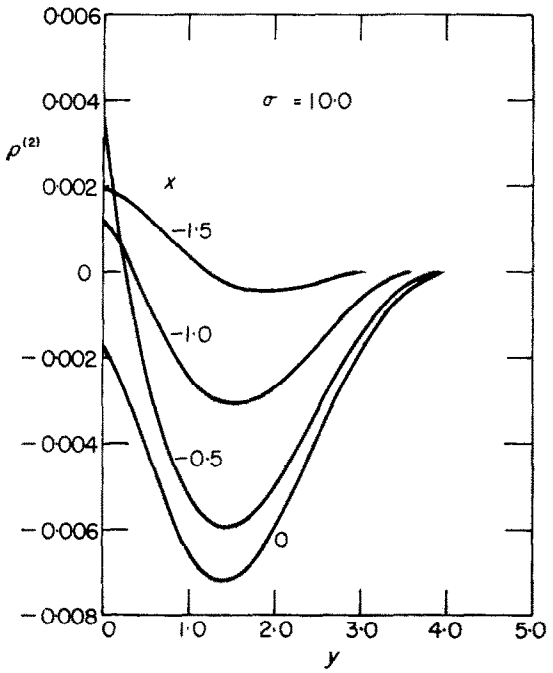

FIG. 7. Second-order pressure perturbation $p^{(2)}$ for Prandtl number 10·0.

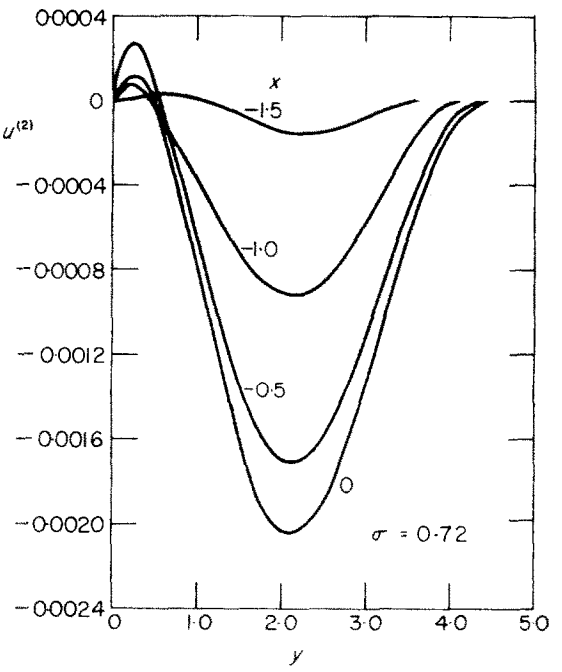

FIG. 8. Second-order normal-velocity perturbation $v^{(2)}$ for Prandtl number 0·72.

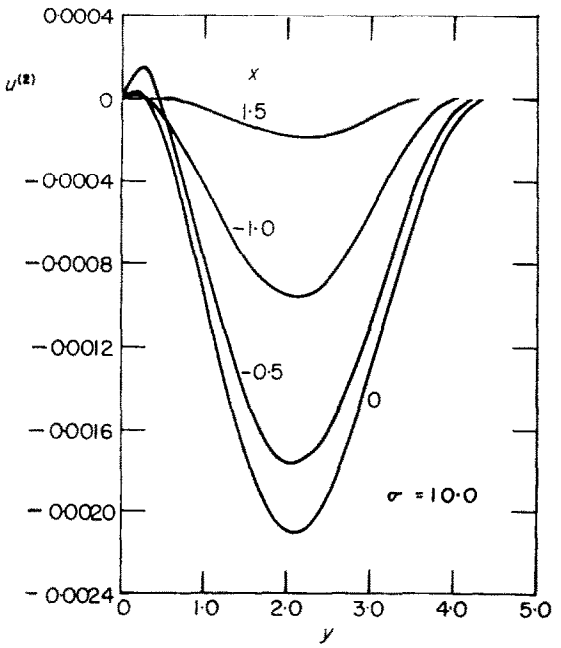

FIG. 9. Second-order normal-velocity perturbation $v^{(2)}$ for Prandtl number 10·0.

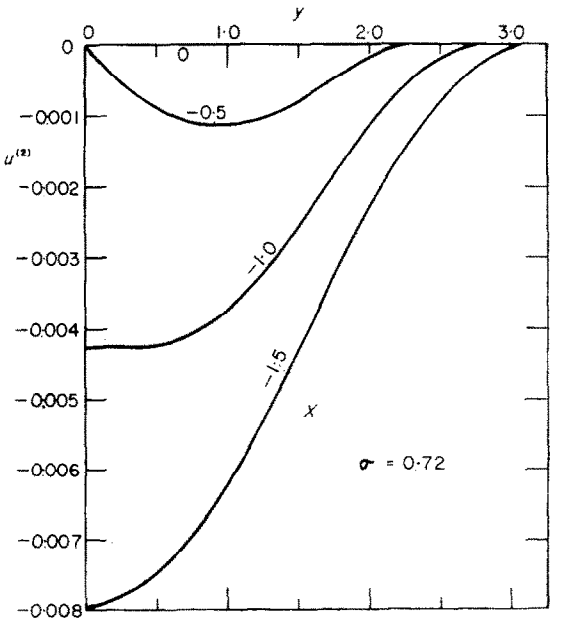

FIG. 10. Second-order velocity perturbation $u^{(2)}$ for Prandtl number 0·72.

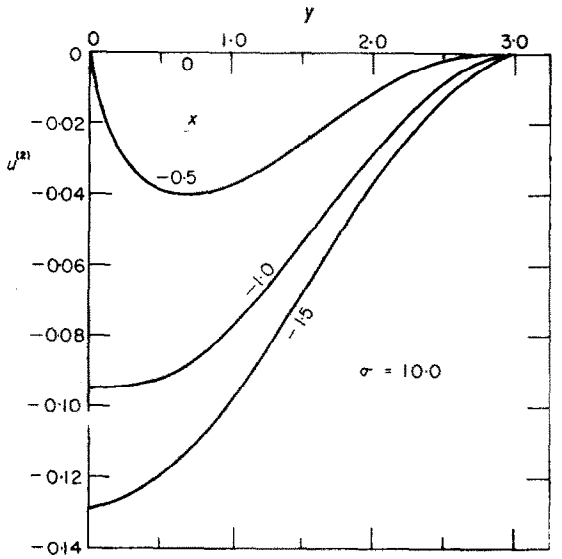

FIG. 11. Second-order velocity perturbation $u^{(2)}$ for Prandtl number 10·0.

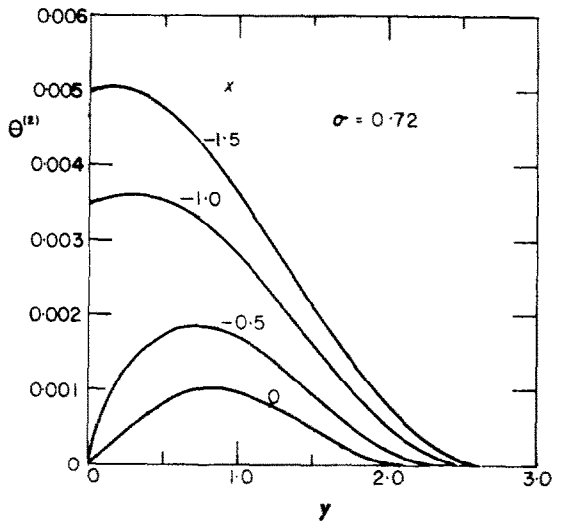

FIG. 12. Second-order temperature perturbation $\theta^{(2)}$ for Prandtl number 0·72.

Since only the zeroth-, first- and second-order approximations are calculated in the present study, the present results, strictly speaking, are only valid up to a Grashof number for which all the perturbation series in equations (11) converge satisfactorily. Even though there is an indication that the convergence of these series is somewhat uncertain at a Grashof number of unity, this

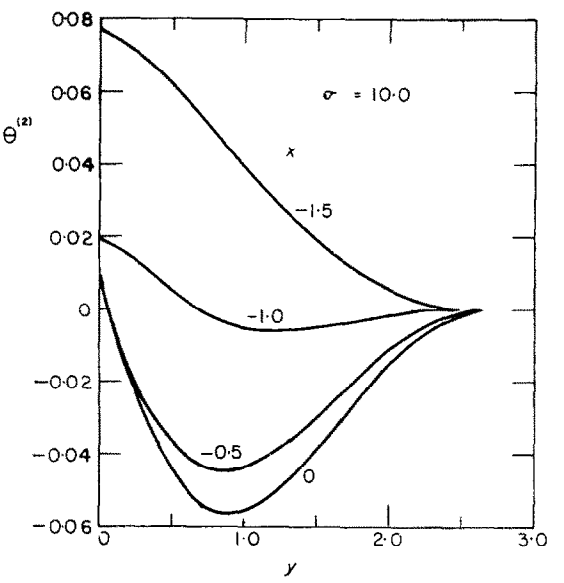

FIG. 13. Second-order temperature perturbation $\theta^{(2)}$ for Prandtl number 10·0.

value is nevertheless taken in the present study as the highest Grashof number to be considered for which the present results are at least qualitatively correct. In the Grashof-number range from zero to unity and for Prandtl numbers of 0·72 and 10·0, the detailed effects of Grashof number on the energy and momentum fields have been evaluated and the results are shown in Figs. 14 to 19. Three essential characteristics are here considered, namely, the temperature field as given by the temperature variable θ, the momentum field by the stream function ψ, and the overall heat-transfer characteristic by the average Nusselt number. These characteristics are now discussed separately as follows.

Figures 14 and 15 show the effect of Grashof number on the temperature field for Prandtl numbers of 0·72 and 10·0, respectively. For the lower Prandtl number, the Grashof-number effect is very slight. Nevertheless, the effect of convection causing the closed isothermal lines to become fuller in the upper-half plane, as the Grashof number increases, can still be seen. This effect, however, becomes much more pronounced in the higher Prandtl-number case. The development of the temperature field, as Grashof number increases, can be dramatically seen in

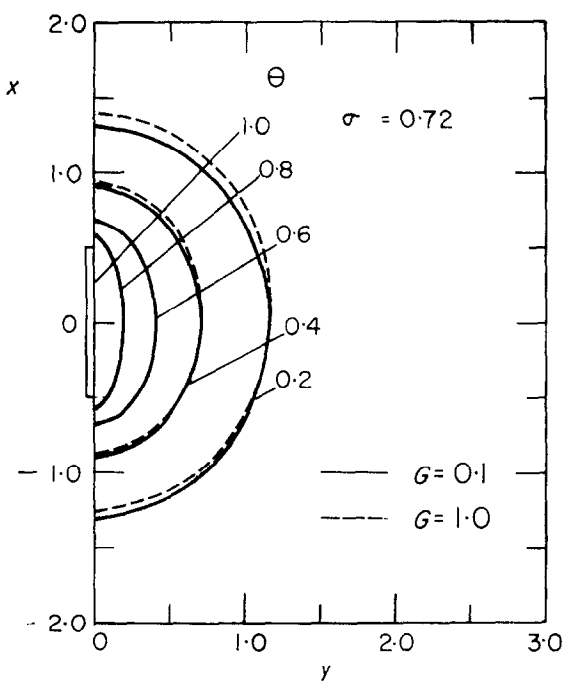

FIG. 14. Temperature field for Prandtl number 0·72.

Fig. 15, where isothermal lines for $G \leqslant 0{\cdot}1$ are not shown, since they become almost identical to those in Fig. 14. However, it should be noted that even at $G = 1{\cdot}0$, the Rayleigh number is already 10·0 at this Prandtl number.

More interesting, perhaps, is the effect of Grashof number on the stream lines. Based on the usual definition of a stream line for viscous flow, the stream function ψ may be conveniently determined from the following equation:

$$\psi(x, y) = \int_0^y u(x, y)\,\mathrm{d}y = \int_0^y (Gu^{(1)} + G^2u^{(2)} + \ldots)\,\mathrm{d}y \qquad (24)$$

It is noted here that the stream line along $y = 0$ is arbitrarily given a value of zero. Several typical stream-line patterns are shown in Figs. 16, 17 and 18. Here for Prandtl number of 0·72, by far the major contribution is due to first-order quantities, which are responsible for the symmetrical nature of the stream lines. This is in complete analogy to that of Stokes flows in forced-flow problems. The second-order approximations start to distort this symmetry, and give quite different flow details in the neighborhood of the leading edge and of the trailing edge of the plate. This, however, is not quite evident in the case of $\sigma = 0{\cdot}72$, as shown in Fig. 16. Figures 17 and 18 present the corresponding stream lines for $\sigma = 10{\cdot}0$ and Grashof numbers of 0·5 and 1·0 respectively. Here the influence of the Grashof number becomes quite apparent. As the Grashof number increases from a small value, the same stream lines in the immediate neighborhood of the plate leading edge spread more and more outward. Since the mass flux between any pair of known stream lines stays the same, spreading out of these stream lines does imply reduced velocities. Presumably, these velocities would decrease further with further increase in Grashof number. This phenomenon is indeed consistent with the boundary-layer behavior at high Grashof numbers, since according to the Pohlhausen's boundary-layer solution, velocities

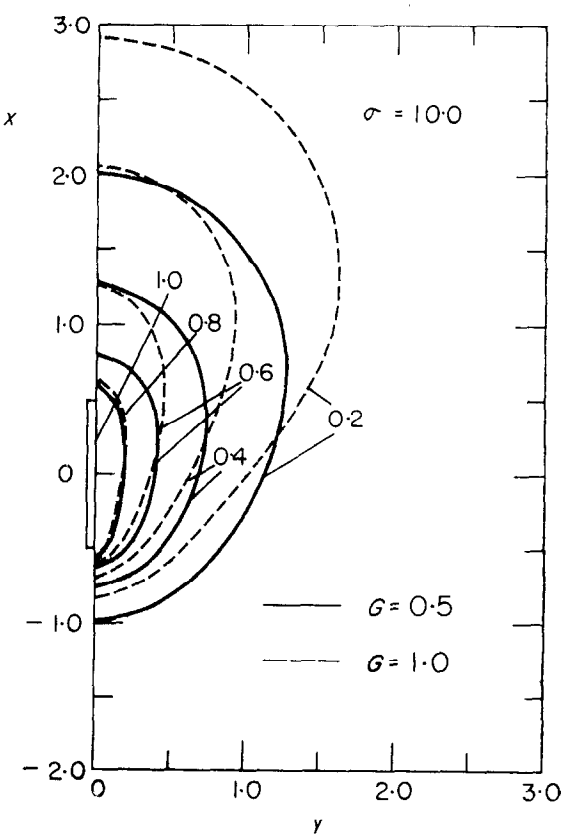

FIG. 15. Temperature field for Prandtl number 10·0.

at locations ahead of the plate are taken to be zero. More significantly, the present calculations show that flow does start ahead of the plate leading edge, as commonly conjectured. Furthermore, even at high Grashof numbers, the flow behavior in the immediate vicinity of the leading edge is that of low Grashof numbers. This leading edge effect, however, is not accounted for in the boundary-layer solution, nor in the boundary-layer perturbation solution [1]. The Grashof number does not seem to affect the flow above the plate in the wake region greatly. The significance of the present results relative to the wake flow is that they account for the proper spreading of the stream lines at large distances away from the plate such that the velocity component u eventually approaches zero as $x \to \infty$, as in contrast to the boundary-layer formulation for the asymptotic wake flow where velocity u along $y = 0$, unrealistically, increases without bound as x tends to infinity.

Finally, the average Nusselt number N calculated from

$$N = \frac{hL}{k} = -\int_{-1/2}^{+1/2} \frac{\partial\theta}{\partial y}\,dx = -\int_{-1/2}^{+1/2} \left[\frac{\partial\theta^{(0)}}{\partial y} + G^2\frac{\partial\theta^{(2)}}{\partial y} + \ldots\right] dx \qquad (25)$$

which is a mere generalization of equation (23), is plotted in Fig. 19 against the usual Rayleigh number or the product of Grashof and Prandtl numbers for Prandtl numbers of 0·72 and 10·0. Note that $(\partial\theta^{(1)}/\partial y)$ does not contribute toward N in view of symmetry. Within the Grashof-number range from zero to unity, the Nusselt

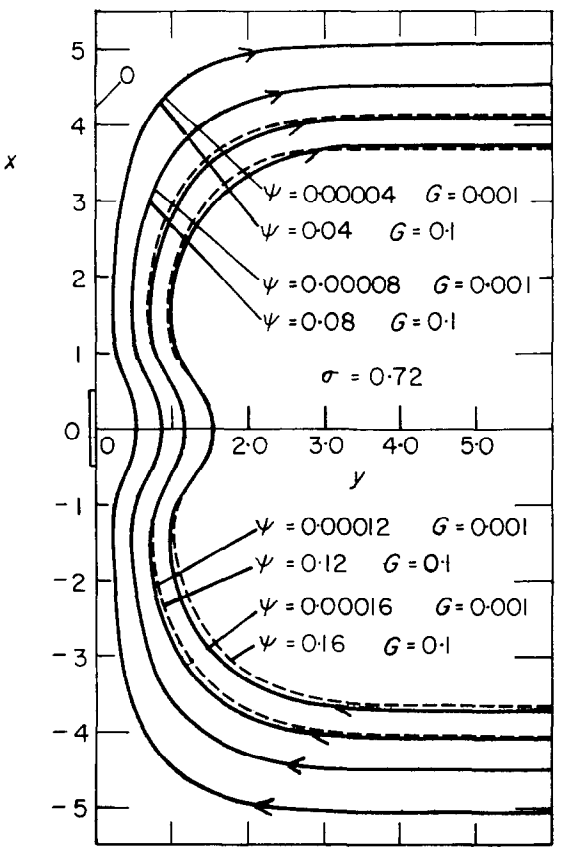

FIG. 16. Stream lines for Prandtl number 0·72.

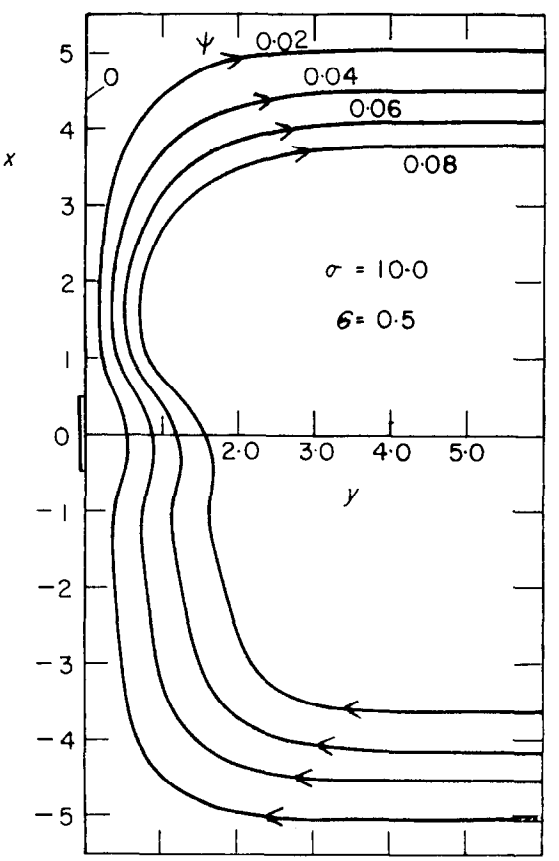

FIG. 17. Stream lines for Grashof number 0·5 and Prandtl number 10·0.

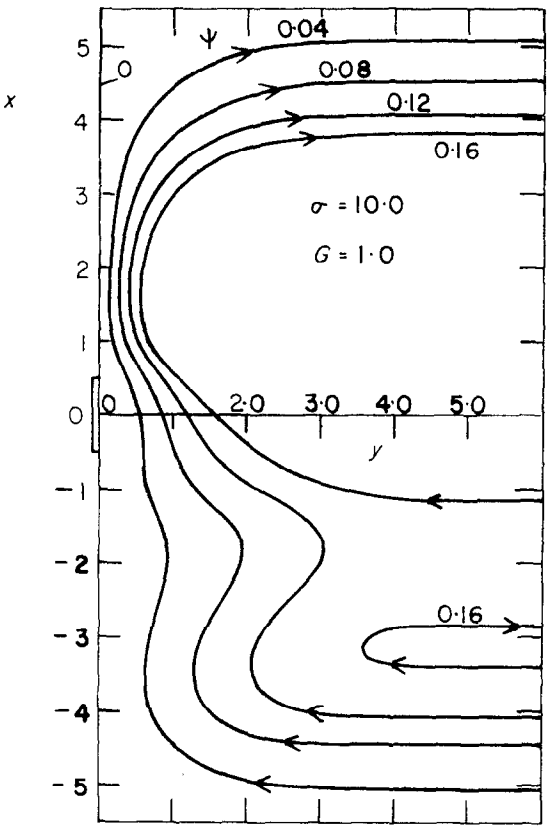

FIG. 18. Stream lines for Grashof number 1·0 and Prandtl number 10·0.

number deviates very little from its limiting value of 1·4413 for Prandtl number of 0·72, while for the higher Prandtl number this deviation starts to become noticeable at $G = 0{\cdot}1$. This is also consistent with the boundary-layer solution at high Grashof numbers where on the same Nusselt number–Rayleigh number plot, the curve for $\sigma = 10{\cdot}0$ also lies above that for $\sigma = 0{\cdot}72$ [1]. Also shown in Fig. 19 are several values from the correlations of McAdams [10] for short vertical plates, and of King [13] for a number of different geometries including the vertical plate. The comparison among the Nusselt numbers is somewhat difficult to interpret, since the present calculations are not expected to be valid beyond a Grashof number of unity and are probably only qualitatively correct at $G = 1{\cdot}0$, and at the same time the experimental correlations become increasingly more uncertain as Grashof number tends to zero.

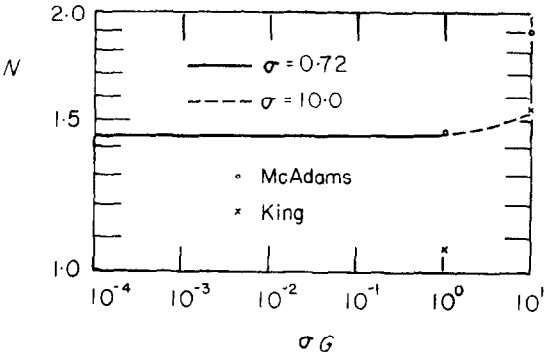

FIG. 19. Nusselt numbers at extremely small Grashof numbers.

LEADING-EDGE CORRECTIONS FOR BOUNDARY-LAYER SOLUTIONS

As mentioned previously, Yang and Jerger [1] have obtained first-order perturbations to the classical Pohlhausen's solution, and shown that their predicted local velocity profiles agree better with the experimental data of Schmidt and Beckmann [2]. However, their corrections on the average Nusselt numbers, though very small, bear a different sign as that suggested by the existing experimental data. It has been conjectured [1] that such a discrepancy could be due to the inadequacy of both the Pohlhausen's solution and the boundary-layer perturbation solution to take into account the leading-edge convection effect. In order to verify this conjecture rigorously, the solution to the present vertical-plate problem must be known for the entire Grashof-number range. However, based on the present results for very small Grashof numbers, it is now possible to estimate the magnitudes of this leading-edge effect toward the average Nusselt numbers. The whole vertical plate is here divided into two regions, the leading-edge region $-\frac{1}{2} \leqslant x \leqslant x_m$ and the boundary-layer region $x_m < x < \frac{1}{2}$. The leading-edge region is characterized by low Grashof-number flow, while the boundary-layer region, by boundary-layer flow with first-order perturbations included. For further simplification, the

local heat-transfer characteristics for low Grashof-number flow are taken to be that given by $\theta^{(0)}$ and $\theta^{(1)}$ only. The location of matching the two regions, x_m, is determined by matching the local coefficients of heat transfer at a specified Grashof number. The local Grashof number used to evaluate the local heat-transfer coefficient in the leading-edge region is calculated on the basis of a local characteristic length $(x_m + 0{\cdot}5)$, which is the distance between the matching point and the plate leading edge. Once x_m is thus determined, the average Nusselt number for the entire plate may then be calculated by integrating the local coefficients in both regions. The results in terms of Nusselt numbers are shown in Table 2, together with corresponding values given by the boundary-layer solutions and the correlations by McAdams [10] and King [13]. It is seen that the leading-edge effect vanishes completely for Grashof numbers greater than 10^8, and becomes more and more significant as Grashof number decreases. Also, the corrections on the boundary-layer values due to the leading-edge effect are much more significant than that due to boundary-layer perturbations. Also of interest is the extent of the leading-edge region at different Grashof numbers. It decreases when the Grashof number increases, as entirely expected. In view of the uncertainty in determining the local Grashof number for the leading-edge region and the lack of knowledge concerning the intermediate Grashof-number range at the present time, the present estimate of the leading-edge effect is by no means conclusive. However, it does indicate that the leading-edge effect could very well outweigh the small negative corrections given by the boundary-layer perturbations.

CONCLUDING REMARKS

In this paper, a perturbation solution to the complete set of governing differential equations for laminar free convection along a finite, isothermal vertical plate in the range of extremely low Grashof numbers and arbitrary Prandtl numbers is presented. Detailed perturbation functions up to and including the second-order approximations have been calculated numerically by the standard relaxation technique for two Prandtl numbers of 0·72 and 10·0. These functions are shown graphically. Also shown are isothermal lines and stream lines illustrating individual effects of Grashof and Prandtl numbers on the energy and momentum fields.

Several more important conclusions may now be summarized. The limiting Nusselt number as

Table 2. Comparison of predicted Nusselt numbers at high Grashof numbers with those from experimental correlations

G		10^4	10^5	10^6	10^7	10^8	10^9
Boundary-layer solution only	$\sigma = 0{\cdot}72$	4·76	8·46	15·04	26·8	47·6	84·6
	$\sigma = 10{\cdot}0$	11·03	19·61	34·86	61·9	110·3	—
Boundary layers with first-order perturbations [1]	$\sigma = 0{\cdot}72$	4·54	8·24	14·82	26·6	47·4	84·4
	$\sigma = 10{\cdot}0$	10·87	19·45	34·70	61·8	110·0	—
Boundary layers with perturbations and leading-edge corrections	$\sigma = 0{\cdot}72$	6·32	8·92	15·32	27·1	47·6	84·6
	$x_m + 0{\cdot}5$	0·277	0·136	0·0725	0·0410	0·0236	0·0139
	$\sigma = 10{\cdot}0$	12·05	20·16	35·22	62·72	110·2	—
	$x_m + 0{\cdot}5$	0·136	0·0735	0·0417	0·0239	0·0137	—
McAdams [10]	$\sigma = 0{\cdot}72$	5·60	9·60	17·0	30·5	54·0	97·0
	$\sigma = 10{\cdot}0$	10·50	18·60	33·1	58·9	105·0	—
King [13]	$\sigma = 0{\cdot}72$	5·40	9·20	16·0	30·0	57·0	112·0
	$\sigma = 10{\cdot}0$	10·00	17·40	33·1	63·1	126·0	—

the Grashof number tends to zero is independent of the Prandtl number, and has a numerical value of 1·4413. As the Grashof number deviates slightly from zero, the momentum field changes from a stationary field to one which varies linearly with the Grashof number, and is also independent of the Prandtl number. In this case, the stream lines are completely symmetrical with respect to the mid-plane of the plate ($x = 0$). As the Grashof number further increases, the closed isothermal lines become fuller in the upper plane and closer to one another in the lower plane. Also, the stream lines tend to spread out in the neighborhood of the leading edge more, while those in the vicinity of the trailing edge of the plate are not greatly affected. All these Grashof-number effects become quite pronounced for Prandtl number of 10·0, as in contrast to the case of Prandtl number of 0·72, for which the above effects are only slightly realized in the Grashof-number range between zero and unity. Finally, it has also been shown that even at high Grashof numbers, the low Grashof-number phenomenon could still play an important enough role as to significantly influence boundary-layer heat-transfer characteristics, especially in the range of moderately high Grashof numbers.

The present analysis and calculations have been carried out for a finite vertical plate. In view of the dimensionless quantities utilized, the results are valid for any finite plate height L. However, when L becomes infinite as in the case of a semi-infinite plate, the wake region completely vanishes and the present results are only expected to describe the physical phenomenon in the neighborhood of the leading edge. This is somewhat different from the boundary-layer formulation at large Grashof numbers, for which the Pohlhausen's solution is valid for both the semi-infinite and finite vertical-plate cases, and in fact, this formulation is also valid in the near-wake region above the finite plate [12]. The present results, however, show that in the far-wake region the boundary-layer behaviors no longer exist.

Finally, it is pertinent to note that, even though the assumptions utilized in the present analysis have been justified in the literature on physical grounds, no detailed experimental data relative to momentum and energy fields in this range of Grashof number are known to permit direct comparison with the present results. In view of the basic nature of this free-convection phenomenon, it is sincerely hoped that such experimental information will become available in the literature.

ACKNOWLEDGEMENT

This study represents part of research on free-convection phenomena sponsored by the National Science Foundation under Grant G-21413 to the University of Notre Dame. Their financial assistance in this study is greatly appreciated.

REFERENCES

1. K. T. YANG and E. W. JERGER, First-order perturbations of laminar free-convection boundary layers on a vertical plate, *J. Heat Transfer* **C86**, 107 (1964).
2. E. SCHMIDT and W. BECKMANN, Das Temperature- und Geschwindigkeitsfeld vor einer Wärme abgebender senkrechter Platte bei naturlicher Konvektion, *Tech. Mech. Thermodynamik* **1**, 341 (Okt. 1930); cont. **1**, 391 (Nov. 1930).
3. M. M. FARZETEDINOV, On the uniqueness of the solutions of the equation of weak convection in the steady state, *Prikl. Mat. Mekh.* **22**, 393 (1958).
4. J. J. MAHONY, Heat transfer at small Grashof numbers, *Proc. Roy. Soc.*, **A238**, 412 (1956–1957).
5. B. L. REEVES and C. J. KIPPENHAN, On a particular class of similar solutions of the equations of motion and energy of a viscous fluid, *J. Aerospace Sci.* **29**, 38 (1962).
6. E. M. SPARROW and J. L. GREGG, Similar solutions for free convection from a nonisothermal vertical plate, *Trans. Amer. Soc. Mech. Engrs* **80**, 379 (1958).
7. D. N. ALLEN, *Relaxation Methods in Engineering and Science*. McGraw-Hill, New York (1954).
8. M. G. SALVADORI and M. L. BARON, *Numerical Methods in Engineering*. Prentice-Hall, New York (1952).
9. M. JAKOB, *Heat Transfer*, Vol. 1, Chapter 25. John Wiley, New York (1949).
10. W. H. MCADAMS, *Heat Transmission*, 3rd Edition, p. 173. McGraw-Hill, New York (1954).
11. V. M. BUZNIK and K. A. BEZLOMTSEV, A generalized equation for the heat exchange of natural and forced convection during external flow about bodies, *Izv. Vyssh. Uchebn. Zavedenu: Energetika* no. 2, 68 (1960); Ref. *Zh. Meckh.* no. 6, Rev. 6*V*506 (1961).
12. K. T. YANG, Laminar free-convection wake above a heated vertical plate, *J. Appl. Mech.* **31**, 131 (1964).
13. W. J. KING, Free convection, *Mech. Engng* **54**, 347 (1932).

Résumé—La convection naturelle laminaire au voisinage d'une plaque finie verticale et isotherme est étudiée dans la gamme de nombres de Grashof entre zéro et l'unité et deux nombres de Prandtl de 0,72 et 10,0, au moyen d'une analyse de perturbation. Les solutions des équations différentielles régissant le phénomène sont exprimées en séries de perturbation; le nombre de Grashof étant pris comme paramètre de perturbation. Trois termes dans tous les développements en séries ont été calculés numériquement en employant la technique de relaxation pour les deux nombres de Prandtl. Les résultats de toutes les fonctions de perturbations, aussi bien que les lignes de courant et les lignes isothermes pour divers nombres de Grashof et les deux nombres de Prandtl sont tracés graphiquement et discutés. Finalement, ces résultats sont employés pour discuter les effets de bord d'attaque relatifs aux solutions bien connues de la couche limite.

Zusammenfassung—Mit Hilfe einer Störungsanalyse wird für den Bereich der Grashofzahlen zwischen Null und Eins und die zwei Prandtlzahlen 0,72 und 10,0 die laminare, freie Konvektion in der nächsten Umgebung einer isothermen, senkrechten, endlichen Platte untersucht. Lösungen der den Vorgang beschreibenden Differentialgleichungen werden in Störreihen, wo die Grashofzahl selbst als Störparameter genommen wird, ausgedrückt. Drei Glieder werden numerisch in allen Reihenentwicklungen unter Verwendung der Relaxationstechnik für beide Prandtlzahlen berechnet. Die Ergebnisse aller Störfunktionen, sowohl der Isothermen wie auch der Stromlinien werden für verschiedene Grashofzahlen und die zwei Prandtlzahlen graphisch dargestellt und diskutiert. Schliesslich werden diese Ergebnisse dazu verwendet, die Einflusse der Vorderkante in Beziehung auf die gut bekannten Grenzschichtlösungen zu diskutieren.

Аннотация—Методами теории возмущений изучается свободная конвекция вблизи вертикальной плоской пластины для чисел Грасгофа от нуля до единицы и двух чисел Прандтля. Решение исходных уравнеиий ищестя в виде рядов по малому параметру, за который принято число Грасгофа. Для обоих значений критерия Прандтля три члена во всех разложениях рассчитаны численно с помощью релаксационного метода. Графически показаны и обсуждаются все результаты, в том числе изотермы, линии тока. Наконец, эти результаты используются для анализа эффектов на передней кромке и сравниваются с хорошо известными решениями пограничного слоя.